Journal of
Plant Ecology

VOLUME 10, NUMBER 1,
PAGES 111–127

FEBRUARY 2017

doi:10.1093/jpe/rtw065

available online at
www.jpe.oxfordjournals.org

On the combined effect of soil fertility and topography on tree growth in subtropical forest ecosystems—a study from SE China

Thomas Scholten[1,*], *Philipp Goebes*[1], *Peter Kühn*[1], *Steffen Seitz*[1], *Thorsten Assmann*[2], *Jürgen Bauhus*[3], *Helge Bruelheide*[4,5], *Francois Buscot*[5,6], *Alexandra Erfmeier*[2], *Markus Fischer*[7], *Werner Härdtle*[2], *Jin-Sheng He*[8], *Keping Ma*[9], *Pascal A. Niklaus*[10], *Michael Scherer-Lorenzen*[11], *Bernhard Schmid*[10], *Xuezheng Shi*[12], *Zhengshan Song*[1,12], *Goddert von Oheimb*[13], *Christian Wirth*[5,14], *Tesfaye Wubet*[5,6] *and Karsten Schmidt*[1]

[1] *Department of Geosciences, Soil Science and Geomorphology, University of Tübingen, Rümelinstraße 19-23, 72070 Tübingen, Germany*
[2] *Institute of Ecology, Leuphana University Lüneburg, Scharnhorststr. 1, 21335 Lüneburg, Germany*
[3] *Faculty of Forest and Environmental Sciences, Silviculture, University of Freiburg, Tennenbacherstraße 4, 79085 Freiburg im Breisgau, Germany*
[4] *Institute of Biology / Geobotany and Botanical Garden, Martin Luther University Halle Wittenberg, Am Kirchtor 1, 06108 Halle, Germany*
[5] *German Centre for Integrative Biodiversity Research (iDiv) Halle-Jena-Leipzig, Deutscher Platz 5e, 04103 Leipzig, Germany*
[6] *Helmholtz Centre for Environmental Research UFZ, Theodor-Lieser-Straße 4, 06120 Halle, Germany*
[7] *Department of Plant Sciences, University of Bern, Altenbergrain 21, 3013 Bern, Switzerland*
[8] *Peking University, No. 5 Yiheyuan Road, Haidian District, Beijing 100871, China*
[9] *Institute of Botany, Chinese Academy of Sciences, No. 20 Nanxincun, Xiangshan, Beijing 100093, China*
[10] *Institute of Evolutionary Biology and Environmental Studies, University of Zürich, Winterthurerstrasse 190, 8057 Zürich, Switzerland*
[11] *Faculty of Biology, Department of Geobotany, University of Freiburg, Schänzlestraße 1, 79104 Freiburg, Germany*
[12] *Institute of Soil Science, Chinese Academy of Sciences, No. 71 East Beijing Road, Nanjing, China*
[13] *TU Dresden, Biodiversity and Nature Conservation, Pienner Straße 7, 01737 Tharandt, Germany*
[14] *Department of Systematic Botany and Functional Biodiversity, University of Leipzig, Johannisallee 21, 04103 Leipzig, Germany*
*Correspondence address. Department of Geosciences, University of Tübingen, Rümelinstraße 19-23, 72070 Tübingen, Germany. Tel: +49-7071-29-72400; Fax: + 49-7071-29-5391; E-mail: thomas.scholten@uni-tuebingen.de

Abstract

Aims

The aim of our research was to understand small-scale effects of topography and soil fertility on tree growth in a forest biodiversity and ecosystem functioning (BEF) experiment in subtropical SE China.

Methods

Geomorphometric terrain analyses were carried out at a spatial resolution of 5 × 5 m. Soil samples of different depth increments and data on tree height were collected from a total of 566 plots (667 m^2 each). The soils were analyzed for carbon (soil organic carbon [SOC]), nitrogen, acidity, cation exchange capacity (CEC), exchangeable cations and base saturation as soil fertility attributes. All plots were classified into geomorphological units. Analyses of variance and linear regressions were applied to all terrain, soil fertility and tree growth attributes.

Important Findings

In general, young and shallow soils and relatively small differences in stable soil properties suggest that soil erosion has truncated the soils to a large extent over the whole area of the experiment.

This explains the concurrently increasing CEC and SOC stocks downslope, in hollows and in valleys. However, colluvial, carbon-rich sediments are missing widely due to the convexity of the footslopes caused by uplift and removal of eroded sediments by adjacent waterways. The results showed that soil fertility is mainly influenced by topography. Monte–Carlo flow accumulation (MCCA), curvature, slope and aspect significantly affected soil fertility. Furthermore, soil fertility was affected by the different geomorphological positions on the experimental sites with ridge and spur positions showing lower exchangeable base cation contents, especially potassium (K), due to leaching. This geomorphological effect of soil fertility is most pronounced in the topsoil and decreases when considering the subsoil down to 50 cm depth. Few soil fertility attributes affect tree height after 1–2 years of growth, among which C stocks proved to be most important while pH_{KCl} and CEC only played minor roles. Nevertheless, soil acidity and a high proportion of Al on the exchange complex affected tree height even after only 1–2 years growth. Hence, our study showed that forest nutrition is coupled to a recycling of litter nutrients, and does not only depend on subsequent supply of nutrients from the mineral soil. Besides soil fertility, topography affected tree height. We found that especially MCCA as indicator of water availability affected tree growth at small-scale, as well as aspect. Overall, our synthesis on the interrelation between fertility, topography and tree growth in a subtropical forest ecosystem in SE China showed that topographic heterogeneity lead to ecological gradients across geomorphological positions. In this respect, small-scale soil–plant interactions in a young forest can serve as a driver for the future development of vegetation and biodiversity control on soil fertility. In addition, it shows that terrain attributes should be accounted for in ecological research.

Keywords: soil fertility, topography, soil erosion, matter transport, biodiversity, DSM, carbon stocks, tree, forest, BEF-China, China

Received: 12 November 2015, Revised: 19 April 2016, Accepted: 17 June 2016

INTRODUCTION

Most theories and concepts of soil formation (Glinka 1927; Hilgard 1914; Jenny 1941; McBratney *et al.* 2003) include the shape of the land surface as essential variable, which has been captured in the catena concept developed by Milne (1935). Topography as a primary terrain attribute is one of the most relevant soil-forming factors. Therefore, geomorphometric variables have been used successfully in numerous studies to predict soil attributes, soil classes and soil formation (e.g. Behrens *et al.* 2014; Hugget 1975; Pennock *et al.* 1987). With regard to soil chemical properties, e.g. Anderson and Furley (1975) found a negative effect of slope angle on soil organic carbon (SOC), nitrogen (N) and pH of topsoil horizons of Chalk soils in Berkshire and Wiltshire Downs in southern England. Wu *et al.* (2013) and Gao *et al.* (2015) found in a forest at Gutianshan National Nature Reserve that elevation of the study plots, SOC, soil moisture and total phosphorous content of the topsoil were important factors shaping the fungal community composition, and soil pH was correlated significantly to microbial biomass (Wu *et al.* 2012). The relationship between soil fertility and slope position has been described for upland soils under a tropical climate in northwest Vietnam (Clemens *et al.* 2010; Wezel *et al.* 2002) with fertile soils occurring on less eroded upper parts of hills. Concerning tree growth, the magnitude of phosphorous (P), N and K fluxes from leaf litter nutrient cycling in a tropical rain forest in Costa Rica varied significantly between Inceptisols with highest average leaf litter concentrations in valleys and Ultisols on slopes and plateaus, which showed lowest concentrations (Wood *et al.* 2006). In addition, terrain attributes were closely related to soil fertility and plant growth when Rossel *et al.* (2010) used visible near-infrared diffuse reflectance spectra of soils to develop a soil fertility index for sugarcane in Sao Paulo State, Brazil. Legendre *et al.* (2009) found in a close-by nature conservation area with comparable geomorphology that topography was a key factor explaining species richness and beta diversity.

The role of topography and soil fertility for tree growth has been described in many studies along large-scale climatic, altitudinal and topography transects (e.g. Griffiths *et al.* 2009; Hairston and Grigal 1991; Homeier *et al.* 2010). The same holds true for landscape-scale studies on the relation between terrain attributes, soil properties, soil classes and pedodiversity (Behrens *et al.* 2010a, b; Schmidt *et al.* 2008; Scholten *et al.* 1997). In general, landscapes with spatially heterogeneous abiotic site conditions provide a greater diversity of soil properties, and thus, offer more niches for different plant and animal species than homogeneous landscapes (Burnett *et al.* 1998; Schmidt *et al.* 2009). However, studies on small-scale heterogeneity of soil properties over distances of tens to hundreds of meters along slopes usually focus on crop land and precision agriculture (e.g. Qin *et al.* 2011; Blasch *et al.* 2015). Only a few studies investigated small-scale effects of elevation or slope position on decomposition (Enoki and Kawaguchi 2000; Gosz *et al.* 1973). Therefore, spatially-explicit analysis of topographic effects on soil fertility and nutrient cycling considering a large number of terrain and landform variables at different scales are rare.

It is clear that abiotic conditions, such as soil fertility, affect individual-tree growth (Baribault *et al.* 2012; van Breugel *et al.* 2011) and thus the productivity of forest stands, but also other ecosystem functions, such as nutrient cycling. More recently, the influence of biodiversity on ecosystem functions such as productivity has been studied intensively, mainly in grassland ecosystems (for recent reviews, see e.g. Cardinale *et al.* 2011; Tilman *et al.* 2014), but also in forests (Nadrowski *et al.* 2010; Scherer-Lorenzen 2014). Although several studies have

documented a significant relationship between tree diversity and functions related to soil properties on a landscape scale, many studies also found strong effects of species identity (Goebes *et al.* 2015a; Li *et al.* 2017; Seitz *et al.* 2016). Such tree growth variations between tree species can be caused by differences in resource use efficiency and allocation patterns (Forrester *et al.* 2006; Riedel *et al.* 2013). However, we assume that local abiotic site conditions are very important for tree growth and may superimpose stand composition and structure (McNab 1989; McKenney and Pedlar 2003; Pretzsch and Dieler 2011; Forrester 2014). Under natural conditions, soil nutrient availability and water availability often showed a high small-scale variability (Boyden *et al.* 2012) and topography is considered to be a major controlling factor (Behrens *et al.* 2014). In this respect, terrain influences the spatial distribution of soil fertility given by SOC, soil pH, cation exchange capacity (CEC) and nutrients (e.g. Officer *et al.* 2004).

Soil fertility as such is not a technical term in soil sciences but describes a soil feature by an interchangeable set of soil properties and soil functions (Patzel *et al.* 2000). In our study, it integrates soil state variables, which characterize soil nutrient supply to plants and provides a framework to differentiate and valuate site conditions for tree growth. In our paper, we apply this framework to a biodiversity and ecosystem functioning forest experiment in subtropical China (BEF China, Bruelheide *et al.* 2011). Therefore, the main objective of this study was to investigate whether topography controls tree growth by small-scale differences of soil fertility expressed in soil texture, soil pH, SOC, N, CEC, base saturation (BS), exchangeable sodium (Na), K, Mg, Ca, Fe and Mn in a hilly forest area in subtropical China. We address three hypotheses about topographic effects on soil fertility and tree growth:

1. Topography affects soil fertility with increasing fertility from ridge to valleys, because of soil erosion processes and matter transport,
2. Individual soil fertility variables are explained by terrain attributes, and
3. Tree growth is positively influenced by soil fertility, and thus also by terrain attributes.

To test these hypotheses, soil fertility attributes and tree height were measured on two experimental sites A and B with 275 and 291 plots, respectively, in SE China, 18.4 and 20.0 ha in size, along a 200 m and 114 m elevation gradient at a spatial resolution of square plots of 667 m^2. Terrain attributes were calculated from a digital elevation model (DEM) with a spatial resolution of 5 × 5 m. BEF-China is the only biodiversity-ecosystem functioning experiment with such a large variation in topography. Thus, this is the first attempt to describe environmental heterogeneity in detail in the context of BEF research.

MATERIAL AND METHODS

Environmental settings

The research area of the BEF experiment established in a highly heterogeneous environment in subtropical China (Bruelheide *et al.* 2011) is located in SE China about 400 km west of Shanghai and situated close to the border between the two counties Dexing (Jiangxi Province) and Kaihua (Zhejiang Province). The two experimental sites A and B of the so-called Main Experiment are located close to Xingangshan Township at the eastern rim of Jiangxi Province (29°08-11 N, 117°90–93 E), China. Both sites belong to the colline altitudinal zone with mean elevations of 189 m a.s.l. (site A) and 137 m a.s.l. (site B) and a mean slope of 25° (site A) and 30° (site B).

Tectonically, both study sites are part of the Neo-Proterozoic Jiangnan belt located between the Yangtze craton in the northwest and the Cathaysia block in the SE, a Neo-Proterozoic orogenic belt (Shu and Charvet 1996) uplifted at about 1000 Ma ago. In the study area, the Middle and Upper Proterozoic sedimentary bedrocks are composed of a series of slightly metamorphosed (greenschist facies) gray-green sandstone, siltstone, and slate deposited between 1400 and 1050 Ma (Lengjiaxi group, Pt2ln) and gray–green and purplish red graywacke, siltstone, sandy slate, and slate (Banxi Group, Pt3bn) deposited between 1000 and 800 Ma ago (Gu *et al.* 2002). Due to rapid uplift of the area since the late Mesozoic (Xiao and He 2005), the structure of the fold-and-thrust belt are characterized by multifold duplexes and individual folds zoned from SE to NW with very steep to almost vertical angles of dip of the sedimentary rocks. Rock outcrops appear at shoulder positions and as spurs. The slopes are typically convex-shaped with inclinations of about <10° in the upper part and 20–35° at midslope positions with more pronounced convexity. The footslopes form the steepest part of the slope with a mean inclination of 30–40° and showed undercutting. Main drainage lines orientate along the striking lines fed by almost orthogonal tributaries that intersect the slopes.

Climatically, the Jiangxi and Zhejiang Provinces belong to the subtropics with moderately cold and dry winters and warm summers. Site A is located on a generally south facing part of a larger mountain chain. Site B is located within a smaller mountain range facing towards east and west. The mean annual temperature is 17.4°C and mean annual rainfall is 1635 mm (Yang *et al.* 2013). The climate of the study area is characterized by subtropical summer monsoon with a wet season from May to July and a dry winter (Goebes *et al.* 2015b, Seitz *et al.* 2015).

Experimental design

After the clear-felling of a *Cunninghamia lanceolata* plantation in 2008 (site A) and 2009 (site B), experimental forests were planted on a plot-level based approach (Bruelheide *et al.* 2014). In total, 40 broad-leaved tree species were planted on 566 plots on a net area of about 38 ha, each measuring 25.82 × 25.82 m (667 m^2), which corresponds to the traditional Chinese unit for area of 1 mu. Per plot, 400 tree individuals were planted in 20 rows of 20 tree individuals each, using a planting distance of 1.29 m. Species were planted in monocultures and mixtures of 2, 4, 8, 16 and 24 species. Species compositions of the different diversity levels

were based on random and trait-informed (non-random) extinction scenarios. The random extinction scenarios were constructed by a broken stick design, starting from three different but overlapping sets of 16 species per site. The first set at each site was subjected to further subplot treatments by planting additional shrub species between tree positions (Very Intensively Studied Plots [VIPs]). For details on the design see Bruelheide *et al.* (2014).

Field methods

Soils were mapped and classified according to IUSS Working Group WRB (2014) and a geomorphological survey including landslides was carried out on both experimental sites (Fig. 1). Soil sampling was split into two parts: horizon-wise sampling for pedogenesis and soil classification using soil pits and schematic sampling conducted by drilling for soil physical and chemical analyses. In 2010 and 2011 on Site A and B, respectively, we sampled nine and seven key soil pits (pedons) and 275 and 291 plots. On each plot, nine soil cores (diameter of 3 cm), were taken to a depth of 50 cm and pooled. Soil cores were bulked to five depth increments (0–5, 5–10, 10–20, 20–30, 30–50 cm) resulting in five soil samples for each plot. Additionally, volumetric samples were taken on all VIP plots in 2014 and 2015 at equal depths for bulk density (BD). Tree height, which is an integral measure of growth performance and commonly used to indicate site quality for even-aged forest stands (e.g. Chen *et al.* 1998; McNab 1989), was determined for the central 6 × 6 trees in the monocultures and two-species mixtures (total = 36 trees) and the central 12 × 12 trees (total = 144 trees) in the 4-, 8-, 16- and 24-species mixtures (Li *et al.* 2014a, 2014b). Data were sampled for site A in September and October 2010 and for site B in 2011. Tree height was determined with a measuring pole as the length from stem base to the apical meristem at every plot (Li *et al.* 2014a).

Laboratory analysis

Soil sample preparation included hand sorting of coarse plant and animal residuals, sieving (<2 mm) and grinding of air-dried soil samples. Particle size analysis was done by combined pipette and sieving method (seven fractions, Koehn, DIN 19683-1) for all soil horizons sampled from

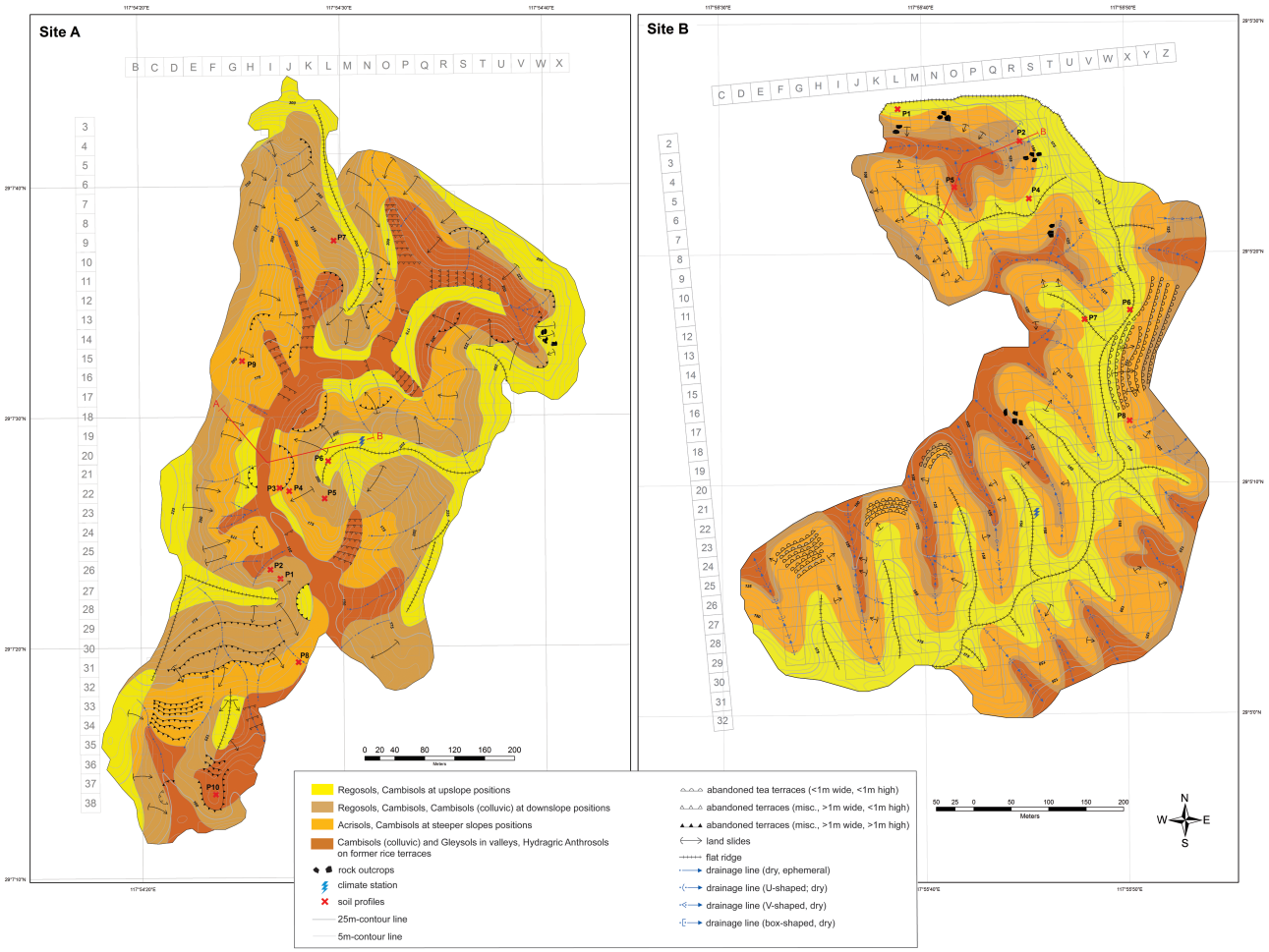

Figure 1: soil-geomorphological map of the experimental sites A (left) and B (right).

the pedons. Soil pH was measured in both 1M KCl and bi-distilled H_2O potentiometrically and was determined for all plot samples. Total organic carbon (TOC) and total nitrogen (TN) were measured with a CN-analyzer (VARIO EL III, Elementar, Hanau, Germany) for all plot samples. Given the acidic soil conditions on both experimental sites, inorganic C does not occur and TOC represents the soil organic carbon content (SOC_{cont}). SOC stocks (t ha^{-1}) to a depth of 50 cm were calculated according to equation 1 (cf. Don *et al.* 2009):

$$SOC_{stocks} = \sum_{i=1}^{n} (Depth_i \times SOC_{cont} \times BD \times (1 - (CM / 100))) \quad (1)$$

where $Depth_i$ is a specific depth increment (m), SOC_{cont} (g C kg^{-1}) represents the SOC content related to the increment, BD (kg m^{-3}) is the mean BD weighted by depth increment lengths, and CM (%) is the fraction of coarse material >2 mm in diameter, estimated following the German guidelines for soil description (Ad-hoc-AG Boden 2005). BD was determined gravimetrically on volumetric samples (five replicated per plot). As BD was sampled only on VIP plots, we used a Random Forest approach (Breiman 2001) to predict BD for all plots on both sites to obtain a consistent data set. CEC and concentrations of exchangeable Na, K, Mg, Ca, H and Al were measured with an ICP-OES (Perkin Elmer DV 5300 ICP OES) for sample from all VIP plots. The soil samples were percolated with an unbuffered 1 M NH_4Cl solution (effective CEC) to assess the potential fertility of the soil. BS percentage was calculated as proportion of the CEC accounted for by exchangeable bases Na, K, Mg and Ca, used as an indication for plant available base cations and soil acidification.

Terrain and landform analysis

A DEM with a cell size of 5×5 m was interpolated from elevation measurements with differential global positioning system (DGPS) using the ordinary kriging algorithm (Krige 1951). Based on the DEM we derived 30 terrain attributes to characterize the local, regional, climatic and complex features of the landscape. To avoid multicollinearity, we chose seven terrain attributes that (i) cover each feature of the landscape at least once, (ii) showed the highest correlation to all soil fertility indicators within each feature (averaging the absolute correlation coefficient over all soil fertility indicators and correlating this value to each terrain attribute) and (iii) are not correlated to each other with $r > 0.7$. The resulting attributes cover the local terrain attributes upstream steepest slope (USSSLP), downstream steepest slope (DSSSLP, both Tarboton 1997), and planform curvature (Zevenbergen and Thorne 1987). The heterogeneity of the terrain is described by the regional terrain attributes terrain ruggedness index (TRI, Riley *et al.* 1999) and relative richness (RR, Behrens 2003). Eastness and northness (Roberts 1986) were used to describe slope aspect indicating plant related climatic conditions. Monte–Carlo based flow accumulation (MCCA, Behrens *et al.* 2008) was used as complex terrain attribute to identify terrain driven water availability. Landform segmentation is based on the concept of openness and geomorphons (Jasiewicz and Stepinsky 2013; Yokoyama *et al.* 2002). These pattern recognition approaches compute elevation differences in the local neighborhood according to the line-of-sight principle and quantify local landform characteristics. The algorithm of Jasiewicz and Stepinsky (2013), which was used here, differentiates between 10 geomorphological units (geomorphons: flat, peak, ridge, shoulder, spur, slope, pit, valley, footslope and hollow). For further processing, we combined depression, flat and valley (resulting in valley) and shoulder, peak and ridge (resulting in ridge) since each of these single geomorphons cover a small number of 5×5 m cells on both experimental sites only. Geomorphons were allocated to plots using the spatial majority of one single unit within a specific plot.

Data analysis and statistical applications

Correlation analyses were done for all terrain and soil fertility attributes using the Spearman correlation coefficient. The influence of terrain attributes on soil fertility were investigated using the residuals of analysis of variance (ANOVA) models that were fitted for each soil fertility attribute used as dependent variable with tree species richness (factor) and tree composition as independent variables to account for treatment effects within the experiment. The adjusted residuals were further used to build linear models that consist of each soil fertility residual as dependent variable and all seven terrain attributes as independent variables. Model simplification was done using the stepwise backward selection method by deleting the least significant variable. CEC, K, Mn, Ca, Mg and BS were log-transformed to obtain normality. In total, we fitted 22 models for 11 soil fertility indicators on both experimental sites ($n_{Site\ A} = 135$, $n_{Site\ B} = 135$).

ANOVA models were used to test for effects of different geomorphological positions (Geomorphons, factor levels: Hollow, Spur, Ridge, Valley (only Site B) and Slope) on soil fertility attributes (dependent variable). We used the residuals of each soil fertility attribute that resulted from the models specified above which accounted for experimental treatments. In case of significant effects of geomorphons, Tukey Honest Significant Differences tests were used to distinguish between different landform segmentations factor levels. Within this approach, we fitted ANOVA models for the topsoil (0–5 cm), the deepest sampled soil depth increment (30–50 cm) and the entire soil (0–50 cm, averaged using depth increment weighted means) on both sites resulting in six models (n of each model = 135). Goodness of fit was measured as the adjusted R-squared.

To identify differences between site A and site B in soil fertility attributes, we fitted each soil fertility attribute against the two-level factor site with tree species richness as fixed and tree composition as random effects (see also Peng *et al.* 2017). To identify the influence of soil fertility and terrain attributes on tree growth, we fitted two linear mixed effect models using all soil fertility and all terrain attributes and tree species richness as fixed variables, respectively and tree species composition as random factors. In those models, tree height was log-transformed.

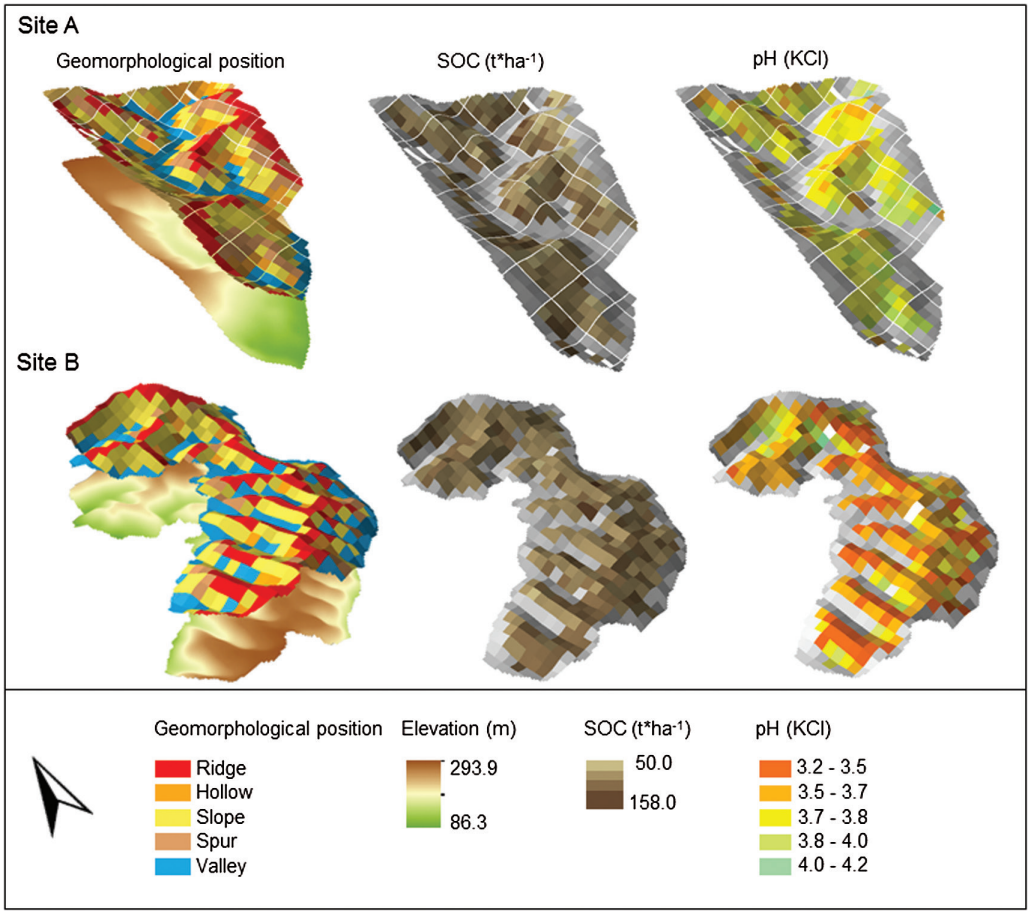

Figure 2: spatial distribution of geomorphological units, soil fertility attributes and C stocks for experimental sites A and B.

For each model, residuals met the requirements of normality and homogeneity of variances after outlier dismission due to cook's distance plots. All analyses were done using R 2.15.3 (R Development Core Team 2013) together with the 'Asreml' package to fit linear mixed effect models (Butler 2009) and the 'RandomForest' package to predict BD (Liaw and Wiener 2002).

RESULTS

Landform analysis

One of the most obvious differences between the two sites is that site A defines a valley while site B comprises a ridge (Fig. 2). The average elevation of site B is about 50 m a.s.l. lower compared to site A. In terms of standard deviation of the elevation values, site B gains only half of the relief energy. Site B showed a more structured relief and topographic heterogeneity (Fig. 2, online supplementary Fig. S1) as revealed by standard deviation (SD) alone and planform curvature cover a much larger range and, together with RR and TRI, showed a higher mean than at site A (Table 1). Furthermore, site B is more exposed to the west with mean values close to zero for northness and eastness as compared to site A with 0.18 for eastness and 0.32 for northness displaying a larger portion of NE facing slopes. MCCA is slightly higher for site B corresponding to slope length and catchment size. The plots at site A do not cover valley positions since the central valley is a swamp land and not part of the Main Experiment while site B has a number of plots in slightly inclined valley cuttings (Figs 1 and 2). The distribution of geomorphological positions across the total area given by geomorphons differs for hollows (site A: 14%, site B: 8%), ridge (site A: 13%, site B 37%), spur (site A: 24%, site B 5%) and valley (site A: 0%, site B 6%). On both sites, slope positions are dominant with 49% at site A and 44% at site B (Fig. 2).

The regular spatial distribution of rectangular experimental plots across a natural surface leads to mixing of members of different geomorphological units within one plot (Fig. 1). Site B contains more such intermediate plots that consist of more than one landform unit because the relief has a higher level of detail. With one well-defined valley situation, fewer small landslides and a larger spatial extent of homogenous surface areas, the delineation of geomorphological units per plot is more precise and unique at site A than at site B.

Table 1: terrain parameters of experimental sites A and B

	Minimum	Maximum	Mean	SD
Site A				
DSSSLP (radiants)	0.19	0.72	0.51	0.11
MCCA ($-\log_{10}$[Sum Px])	0.87	4.47	2.25	0.73
RR (%)	0	30.90	21.46	4.82
TRI (m)	0.72	3.82	2.53	0.66
Eastness (–)	−1.00	1.00	0.18	0.68
Northness (–)	−1.00	1.00	0.32	0.58
Planform curvature (rad m^{-1})	−3.04	2.83	0.25	0.99
Site B				
USSSLP (rad)	0.18	0.81	0.52	0.13
MCCA ($-\log_{10}$[Sum Px])	0.91	3.91	1.77	0.62
RR (%)	21.40	56.58	35.93	7.61
TRI (m)	1.20	4.44	2.80	0.65
Eastness (–)	−1.00	0.99	0.05	0.64
Northness (–)	−0.96	1.00	−0.04	0.57
Planform curvature (rad m^{-1})	−4.37	5.47	0.55	2.02

Abbreviations: MCCA = Monte–Carlo based flow accumulation expressed as the sum of pixels above each pixel of the DEM; TRI = topographic roughness index, planform curvature after Zevenbergen and Thorne.

Key soil profiles (pedons)

The soils cover the reference soil groups Regosols, Cambisols, Acrisols, Gleysols and Anthrosols (Fig. 1, IUSS Working Group WRB 2014), with Cambisols and Regosols on ridges, spurs and crests, Cambisols and Acrisols along slopes and colluvic Cambisols and Gleysols predominantly on footslopes and in valleys. Additionally, hydragric Anthrosols (paddy soils) are present in some valley cuttings and on lower footslopes (Fig. 1). Most soils are qualified as dystric, having a BS below 50%, and siltic with silt contents of 50.0% at site A and 43.5% at site B (online supplementary Table S1). At site A, brownish to yellowish Munsell soil colors dominated, whereas the soils at site B showed more reddish colors (online supplementary Table S1). Hydragric Anthrosols were located on abandoned rice terraces and terrace remnants indicative of past human activity. They have been modified profoundly through human activities, such as addition of organic materials or household wastes, and cultivation. Soil depth increases typically from several centimeters at steep upslope positions, on ridges and on spurs to more than 200 cm at downslope positions, in hollows and in valleys (online supplementary Table S1). The mean soil thickness, calculated as depth to the upper boundary of the C-horizon, was 66 cm at site A and more than double at site B with 143 cm.

In relation to the wide distribution of Jurassic sand and silt stones, the substrate composition, as well as the particle size distribution of all pedons on both experimental sites were quite similar having loam as the main texture class (online supplementary Table S1). Only at site A, a small NNW/SSE facing band represented by pedon 7 (online supplementary Table S1) showed distinctly lower clay and higher silt contents for all soil horizons. The main heterogeneity is related to the thickness of the soil cover (online supplementary Fig. S1) and downslope-increasing C contents, especially at site A (Fig. 2). Soil erosion led to a transport of topsoil material and soil components from ridge to valley positions. However, colluvial sediments were missing widely due to the convexity of the footslopes caused by uplift and removal of eroded sediments by adjacent waterways. Therefore, colluvial sediments occurred only in valleys and on concave footslopes connected to small valley incisions like pedons 2, 5, 8 at site B (Fig. 3). They showed higher C contents of about 1% below 50 cm depth (Table 1). Landslides are a common geomorphic feature at both experimental sites (Fig. 1) forming hollows and small spurs.

Soil fertility attributes

The soils are generally acidic at both experimental sites varying for pH_{KCl} values from 3.2 to 4.7 and pH_{H2O} from 3.9 to 6.0 (online supplementary Table S1). In general, soils at site B are more acidic than soils at site A with lower values of about 0.3 pH units (online supplementary Table S2). At site A, soil pH values showed a slight decrease with increasing elevation, whereas such a trend was not observed at site B (Fig. 2). Even though we measured nearly the same range of pH units for both experimental sites, the spatial extent of very acidic plots is much higher at site B with 37% of the area covered by ridges compared to site A with 13% only. Low pH values are typically accompanied by high exchangeable Al contents ($r = 0.7$).

Exchangeable bases were dominated by bivalent cations (online supplementary Tables S1 and S2) with maximum values of 53.2 (site A) and 52.8 $\mu mol_c\ g^{-1}$ (site B) for Ca and 32.5 (site A) and 11.0 $\mu mol_c\ g^{-1}$ (site B) for Mg. Potassium concentrations were slightly higher at site A compared to site B with a maximum of 3.2 $\mu mol_c\ g^{-1}$ for all VIP plots. Sodium was negligible with maximum values below 2 $\mu mol_c\ g^{-1}$ and a mean of 0.4 and 0.1 $\mu mol_c\ g^{-1}$ at site A and site B, respectively. Contrary to Ca and K, Mn reaches higher values at site B compared to site A while Fe does not differ between both sites. Al is the dominant cation of the exchange complex of the soils accounting for 71% of the CEC at site A and significantly more, 84%, at site B. Together with high H concentrations of 1.7 (site A) and 3.1 $\mu mol_c\ g^{-1}$ (site B), the low BS (18.8% and 8.4%, respectively) reflects strongly acidic soil conditions accompanied by a limited availability of Ca, Mg, Na and K. The CEC is almost equal at both experimental sites.

Generally, C and N contents are highest in the upper 5 cm of the soil and decrease continuously with depth at both sites (Fig. 3, online supplementary Tables S1 and S2). The pedons at site A showed slightly higher C and N contents (4.9% to 2.7% for C, 0.5% to 0.2% for N) in A horizons and within the upper 40 cm of the soil compared to site B. One outlier (site A P06, 10.7% C) may have been caused by incorporation of material from the humus layer during sampling. The mean

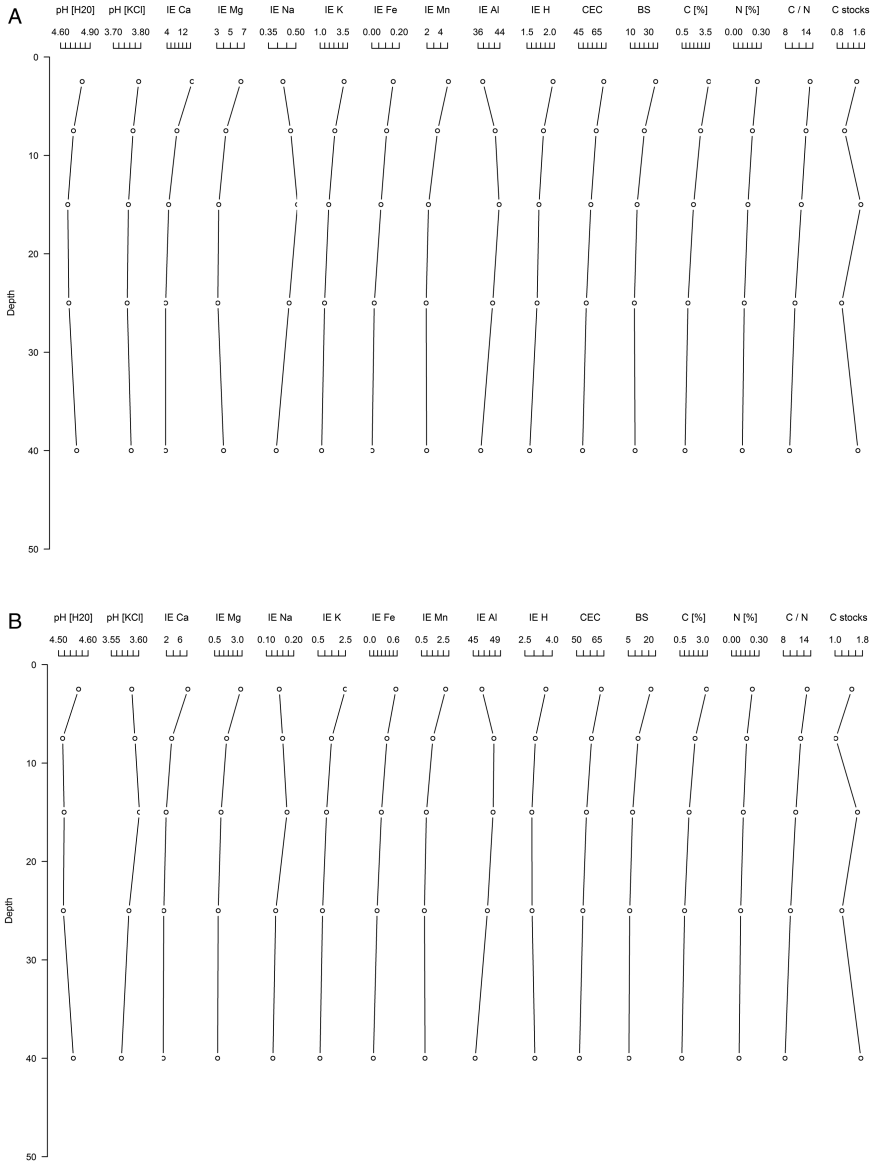

Figure 3: depth functions of soil fertility attributes on both experimental sites.

C contents of the upper 50 cm of all plots (1.7% at site A significantly higher than 1.3% P B) and a uniform BD of 1.3 g cm^{-3} results in mean C stocks of about 70.0 t ha^{-1} on both experimental sites. According to the small variability in BD, the spatial distribution of soil C content and C stocks coincide within the upper 50 cm (Fig. 2), with stocks showing an overall range from 50.0 to 150.8 t ha^{-1}. C stocks are lower on ridges and upper slopes than in hollows and valleys.

Terrain attributes and landform characteristics

Generally, all local terrain attributes showed significant relationships to soil fertility (Table 2). The majority of the 11 fertility attributes is closely related to planform curvature (eight at site A and six at site B). Slope significantly explains eight fertility attributes at site B, but only N at site A. MCCA as complex terrain attribute to identify terrain driven water availability and potential overland flow was of equal importance as planform curvature (six at site A and seven at site B). In contrast to all other fertility attribute, the spatial distribution of C/N ratio was not explained by any terrain attribute and CEC had only a weak relationship to relief at site A. Both regional terrain attributes RR (0 at site A and three at site B) and TRI (three on each site) had minor influence on the spatial distribution of soil fertility distribution. Due to the overall exposure of the experimental sites, northness played a more pronounced role at site A and eastness at site B.

Comparable to terrain attributes, typical landform segments clearly differentiate soil fertility on both experimental sites. Taking the residual of the ANOVAs (Fig. 4), ridge and spur positions were significantly different from

Table 2: results of multiple linear regressions (MLR) using soil fertility attributes as dependent and terrain attributes as independent variables for site A and site B

	pH	pH	IE Ca	IE K	IE Mn	CEC_{eff}	BS	C_{org}	N	C/N	C-stock
	H_2O	KCl	[$\mu mol_c\ g^{-1}$]				[%]	[mass−%]			
Site A											
DSSSLP (radiants)	NS	NS	NS	NS	NS	NS	NS	NS	0.003***	NS	NS
MCCA (−$\log_{10}$[Sum Px])	0.032***	0.011***	0.003**	NS	0.043***	NS	0.026***	NS	−0.003***	NS	NS
RR (%)	NS	NS	NS	NS	NS	NS	NS	NS	NS	NS	NS
TRI (m)	NS	NS	0.026*	NS	NS	NS	0.033*	NS	0.016**	NS	NS
Eastness (−)	NS	NS	NS	NS	NS	NS	NS	NS	NS	NS	NS
Northness (−)	NS	NS	NS	NS	NS	−0.013*	NS	−0.049*	−0.038*	NS	−0.239*
Planform curvature (radiants m^{-1})	NS	−0.015*	0.123**	−0.057***	−0.089**	NS	−0.082**	−0.068***	−0.074***	NS	−0.649***
Site B											
USSSLP (radiants)	0.005***	0.042***	NS	0.137**	0.277***	0.0009***	0.035***	0.055***	0.003***	NS	NS
MCCA (−$\log_{10}$[Sum Px])	0.075***	0.051***	0.247***	0.068*	0.286***	−0.050***	0.223***	NS	0.0005**	NS	NS
RR (%)	NS	−0.023**	NS	NS	−0.126**	NS	−0.041*	NS	NS	NS	NS
TRI (m)	NS	NS	NS	−0.083***	NS	NS	−0.004***	NS	NS	0.137*	NS
Eastness (−)	0.018*	NS	0.073**	NS	0.099***	NS	0.059***	NS	NS	NS	NS
Northness (−)	NS	NS	NS	NS	NS	NS	−0.004*	NS	NS	NS	NS
Planform curvature (radiants m^{-1})	NS	NS	NS	−0.019***	0.065***	−0.009***	−0.017***	NS	−0.004*	NS	−0.212*

It was accounted for the experimental treatments tree species richness and tree species composition before fitting the MLR models for each soil fertility attribute.
*$P < 0.05$, **$P < 0.01$, ***$P < 0.001$.
Abbreviations: MCCA = Monte Carlo based flow accumulation expressed as the sum of pixels above each pixel of the DEM; NS = not significant.

all other segments, except for C/N ratios and C stocks, which were distributed evenly over all landforms (Table 3). Interestingly, slopes tended to show similar behavior for soil fertility attributes as hollows and valleys, except for K at site B.

This overall spatial pattern applies to the total upper 50 cm of the soil and was also valid for specific depth increments of CEC on both experimental sites (Table 3, CEC not affected by geomorphological position at site A, but affected at site B for all depth increments). However, all other soil fertility attributes showed a depth-specific effect, which can explain up to 48% of the spatial distribution. This relation to geomorphons is confirmed for soil pH and exchangeable K only for 0–5 cm at site A. Differences between the experimental sites were best explained by exchangeable base cations Na, Ca, Mg and BS, with higher values at site B than at site A.

Both soil fertility and terrain attributes affected tree height (Table 4). Tree height was significantly related to C stocks at both sites while pH_{KCl}, Mn and CEC affected tree height only at site A. MCCA and planform curvature as terrain attributes affected height growth at both sites while the geomorphological position showed an effect on tree height only at site A. At the time of this study, trees height was on average 120 cm (SD = 65.1 cm) and 74 cm (SD = 28.9 cm) at site A and site B, respectively.

DISCUSSION

Small-scale environmental gradients along land surfaces affects soil fertility

The topography of the study area reflects the geological and geomorphological history of folded sedimentary and slightly metamorphosed rocks. This might explain the much higher silt content in pedon 7 at site A representing a silty phase during sedimentation of the slates which is now exposed to the surface as narrow folding band. Joints are filled with siliceous-rich material, mainly quartz. Since slates weather easily under subtropical climate conditions and quartz is much more resistant to weathering (e.g. Scholten 1997), several cm-thick quartz veins cross the strongly isomorphic weathered slate (saprolite) shaping the large number of ridges and long spurs on both sites with 37% of the total area at site B and 42% at site B (Fig. 2). At site B, the higher values for RR and TRI compared to site A and the reddish Munsell colors of the soils (online supplementary Table S1) indicate that this site has been exposed to weathering processes for a longer time (Giaccio *et al.* 2002) supported by its lower height above sea level as a result of denudation and thus older land surface.

Typically situated at midslope positions, landslides affected substrate thickness and inclination with gently sloping flat surfaces and steep shoulders at the tear-off edge and

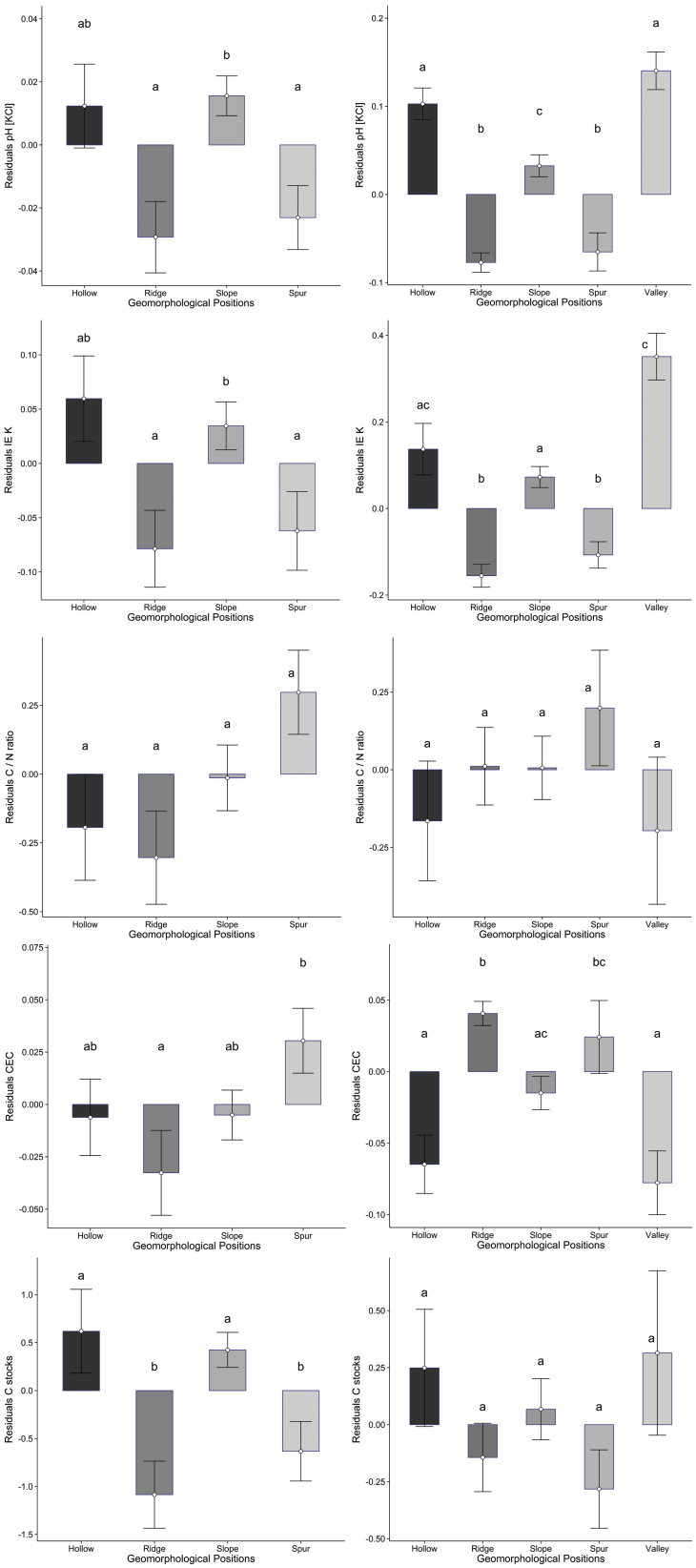

Figure 4: residuals of soil fertility attributes related to geomorphological position for both experimental sites (IE K: ion equivalent of potassium, C: carbon, N: nitrogen, CEC: cation exchange capacity).

Table 3: results of ANOVA using soil fertility attribute residuals as dependent and geomorphological units (factor with four and five different units for site A and site B, respectively) as independent variable for two depth increments and the complete profile

	Depth 0–5 cm		Depth 30–50 cm		Depth 0–50 cm	
	Geomorph. unit	Expl. SS [%]	Geomorph. unit	Expl. SS [%]	Geomorph. unit	Expl. SS [%]
Site A						
pH KCl	***	25	NS	—	**	12
pH H_20	***	19	NS	—	NS	—
IE Ca [$\mu mol_c\ g^{-1}$]	***	13	*	7	***	17
IE K [$\mu mol_c\ g^{-1}$]	***	13	NS	—	*	8
IE Mn [$\mu mol_c\ g^{-1}$]	NS	—	***	13	***	18
CEC_{eff}	NS	NS	*	7	*	5
BS [%]	***	26	NS	—	***	18
C_{org} [mass–%]	*	7	***	16	**	10
N [mass–%]	NS	—-	***	25	***	24
C/N	***	27	*	8	NS	—
C stocks	*	8	***	14	***	14
Site B						
pH KCl	***	47	***	41	***	46
pH H_2O	***	44	***	26	***	36
IE Ca [$\mu mol_c\ g^{-1}$]	***	20	***	35	***	39
IE K [$\mu mol_c\ g^{-1}$]	***	32	NS	NS	***	40
IE Mn [$\mu mol_c\ g^{-1}$]	***	36	***	43	***	48
CEC_{eff}	***	19	***	16	***	23
BS [%]	***	41	***	43	***	48
C [mass–%]	**	11	***	25	NS	—
N [mass–%]	NS	—	***	32	***	25
C/N	***	32	*	8	NS	—
C stocks	***	16	***	17	NS	—

Explained Sum of Squares (Expl. SS) were calculated as percentage of total Sum of Squares.
*$P < 0.05$, **$P < 0.01$, ***$P < 0.001$.
Abbreviations: NS = not significant; — = not calculated.

the lid of the landslide. At the scale of investigation, they interfere with slope formation caused by uplift and erosion over longer periods of time and can explain the high SD for most soil fertility attributes along slopes (online supplementary Table S2) and the irregular small-scale distribution of C at site B (Fig. 2). Also Zhang *et al.* (2012) found such a scattered spatial distribution for soil pH, C and N mainly affected by terrain convexity in a broad-leaved forest in Tiantong, Zhejiang Province, geologically belonging to the Neo-Proterozoic Jiangnan belt, as well as the experimental sites of BEF China.

Significant interrelationships between soil fertility and topography could be discovered by geomorphons (Table 3). In general, site A showed a more heterogeneous distribution of terrain attribute while site B was predominated by ridge positions (37% of the total area). Furthermore, many plots at site B belong to more than one specific geomorphon with high SD for terrain attributes. This is especially true for plots that cover both footslope and valley positions. Thus, site A showed a more precise image of how soil fertility attributes are related to terrain attributes since plot sizes of a regular grid without gaps were too large for the higher geomorphological heterogeneity at site B.

However, minor soil formation and relatively small differences in stable soil properties on both experimental sites suggest that soil erosion has truncated the soils largely over the whole area of the experiment. Soil horizonation processes such as advanced mineral weathering, clay translocation and ferralitization, which are typical for subtropical environments, are missing. Even if soil formation processes are generally proceeding at fast rates in this subtropical environment (IUSS Working Group WRB 2014), soil formation is still young and stable soil attributes like particle size distribution and BD vary only slightly (Fig. 3). Generally, the geomorphological units represent the recent function of relief for matter translocation processes rather than terrain attributes, which reflect small-scale redistribution of soil fertility attributes within such units (Table 2). The cumulated appearance of colluvic Cambisols on footslopes and weakly developed Regosols, as well as the scarce appearance

Table 4: results of the linear mixed effect model for tree height against soil fertility attributes, terrain attributes and geomorphological positions on site A and site B

	pH	IE Ca	IE Mg	IE K	IE Mn	CEC_{eff}	BS	N	C/N	C stocks
	KCl	[$\mu mol_c\ g^{-1}$]					[%]	[mass–%]		
Site A	$F_{1,89} = 4.22^{*}$	$F_{1,87} = 2.39$, NS	$F_{1,83} = 1.25$, NS	$F_{1,88} = 0.02$, NS	$F_{1,86} = 4.31^{*}$	$F_{1,87} = 5.64^{*}$	$F_{1,87} = 3.19$, NS	$F_{1,90} = 1.17$, NS	$F_{1,89} = 0.25$, NS	$F_{1,83} = 7.22^{**}$
Site B	$F_{1,73} = 0.13$, NS	$F_{1,73} = 0.21$, NS	$F_{1,75} = 1.31$, NS	$F_{1,71} = 2.44$, NS	$F_{1,83} = 2.42$, NS	$F_{1,80} = 0.15$, NS	$F_{1,76} = 1.52$, NS	$F_{1,72} = 5.57^{*}$	$F_{1,71} = 1.15$, NS	$F_{1,73} = 3.48^{****}$
	DSSSLP/USSSLP	MCCA	RR	TRI	Eastness	Northness	Planform curvature			
Site A	$F_{1,189} = 0.50$, NS	$F_{1,178} = 5.70^{*}$	$F_{1,184} = 1.00$, NS	$F_{1,178} = 1.10$, NS	$F_{1,186} = 0.20$, NS	$F_{1,187} = 0.80$, NS	$F_{1,173} = 11.70^{***}$			
Site B	$F_{1,185} = 2.00$, NS	$F_{1,178} = 3.40$	$F_{1,200} = 0.80$, NS	$F_{1,199} = 0.01$, NS	$F_{1,190} = 0.90$, NS	$F_{1,195} = 6.80^{**}$	$F_{1,182} = 8.20^{**}$			
	Geomorphological position									
Site A	$F_{3,176} = 8.8^{***}$									
Site B	$F_{4,190} = 1.3$, NS									

Tree species richness was used as fixed and plot composition was used as random factor.
$^{*}P < 0.05$, $^{**}P < 0.01$, $^{***}P < 0.001$, $^{****}P < 0.1$.
Abbreviations: MCCA = Monte Carlo based flow accumulation expressed as the sum of pixels above each pixel of the DEM; NS = not significant.

of further developed Acrisols underpin the actual influence of erosion processes. In valleys, the natural and man-made (former paddy soils from rice cultivation) influence of surface and groundwater forms gleyic properties.

A gently sloping relief with predominantly steep inclinations from 25° to 30° characterizes the study area. Many forest stands on such slopes have been cleared during the Great Leap Forward in the 1950s followed by severe soil erosion in particular in SE China and probably earlier periods of felling (e.g. Aldhous 1993; Huang 1987; Schönbrodt *et al.* 2013; Wang *et al.* 2005). The experimental sites might inherit such erosion pattern especially for SOC stocks at site A (Fig. 2). If we assume an erosion potential of 0.3–3.4 cm yr^{-1} after felling in humid subtropical regions (Jien *et al.* 2015), a mean topsoil SOC content of 2% (online supplementary Table S2), and 2 years' time between felling and soil sampling at both experimental sites, about 1.8–20.4 t ha^{-1} SOC could have been eroded since the establishment of the main experiment. In this respect, soil erosion explains the concurrently increasing CEC and SOC stocks along slopes, in hollows and in valleys, where deprotonating of carboxyl groups provides additional CEC. With an overall mean of 67.8 t ha^{-1} (site A) and 71.2 t ha^{-1} (site B) for the top 50 cm (25.9 and 25.1 t ha^{-1} for 0–10 cm and 52.7 and 53.7 for 0–30 cm, respectively), the recent SOC stocks are distinctly lower than for soils under forest in China in general. They showed 137.3 t ha^{-1} SOC for average soil depths of 75–88 cm, with 54.8 t ha^{-1} in surface soil horizons and 82.5 t ha^{-1} in subsurface soil horizons (Xie *et al.* 2007). Analyses of soils in subtropical forest plantations in China (e.g. monocultures of *Pinus massoniana*, *Castanopsis hystrix*, *Michelia macclurei* and *Mytilaria laosensis*) showed SOC stocks of 56–68 t ha^{-1} for the upper 30 cm (Wang *et al.* 2010). Subtropical hammock ecosystems at MacArthur Agro-ecological Research Centre, Florida, store about 34 t ha^{-1} (0–10 cm, Frank *et al.* 2012). Significant depth gradients and slope gradients both affected SOC stocks on slopes in *C. Lanceolata* stands in near-by Zhejiang Province, where the upper 40 cm of the soils accounted for 55% of the total C storage of 100 cm soil depth and significant differences in SOC stocks were measured for upper and lower slopes (Xue *et al.* 2012). The moderate SOC stocks at both experimental sites suggest that accumulation of SOC has taken place in a considerable amount since the last erosion events. The stable SOC turnover rate at MacArthur of 59 years suggest that the depletion of SOC in the soils of the experimental sites of BEF China by severe soil erosion cannot be explained by recent erosion events after the last felling and the establishment of the main experiment alone but should be inherited from former land use systems to a certain extent. It can be expected that the experimental forest will supply the soil with organic carbon over time at high rates through litter and fine roots (Sun *et al.* 2017; Bu *et al.* 2017). Near-by ecological service forests in Zhejiang Province stored 54 to 89 t C ha^{-1} in their biomass (Zhang *et al.* 2007).

Individual soil fertility attributes are specifically related to terrain attributes

The presence of hollows and spurs significantly affects hydrologic and sedimentary processes like hillslope discharge (O'Loughlin 1973). Since the total proportion of these landforms are equal for both sites (14% of the total area), the extent of eroded area is supposed to be similar and explain the only small differences (less than 0.5 times) between the experimental sites for C stocks, C/N ratio and CEC (Fig. 2, online supplementary Table S2). However, planform curvature or transverse curvature across slope direction covers a wider range and is much higher at site B. Discharge and erosion are more pronounced and explain the occurrence of deposition areas in valley positions as a typical geomorphological feature of site B. Higher rates of potential overland flow at site B given by MCCA support this finding. We assume that leaching and downslope interflow transported base cations downslope followed by accumulation on concave footslopes, in hollows and in valleys. This leads to distinctly lower K, Mg, Ca and Mn contents on ridge and spur positions (for K see Fig. 4). Especially at site B, exchangeable Mg and Ca is almost double in hollows and valley compared to ridge, spur and slope positions where these cations replace Al and H at the exchange complex. Further, desorption of these cations fixed on soil particles can result in significant loss of base cations from the catchment (Pacès 1985). Although a natural process in forest soils, depletion of base cations can be accelerated by harvest and leaching especially under acidic deposition (Huntington 2003), a process that was shown for the Hubbard Brook Experimental Forest (Bormann and Likens 1966) and many other forest ecosystems like the Solling Region in Germany (Matzner and Ulrich 1981) and the Strengbach catchment in NE France (Stille *et al.* 2009). However, some of the mobilized K, Ca, Mg and Mn might be absorbed by vegetation and partly returned to the soil through canopy leaching and litter decomposition as part of a closed plant-soil nutrient cycle (Likens *et al.* 1996; Perakis *et al.* 2006; Poszwa *et al.* 2000).

Among others, already Jenny (1941) stated that topography modifies the water relationships in soils to a considerable extent, and influences soil erosion and thus soil depth. Plots on ridges and spurs have a very low contributing area and limited depth and may suffer both from nutrient leaching and from water shortage during dry and hot periods of the year. Matter transport along slopes is likely for K on both experimental sites were K contents are significantly related to topography in the upper depth increment (0–5 cm), but decreased with increasing soil depth (Table 2). Such depth-dependend relationships between terrain attributes and soil nutrients were also observed for total N and P in soils of mixed forests of *Pinus tabuliformis* and *Quercus aliena* var. *accuteserrata* in Qinling Mountains (Wu 2015). The significant correlation of soil pH with MCCA at site A indicates that matter fluxes by interflow control spatial differences of soil acidity more than CEC (Table 2). Ridge and spur are higher in elevation compared to all other geomorphons of site A and site B. Leaching and downslope transport of base cations led to favorable soil conditions for tree growth in adjacent geomorphons at lower elevations. These processes explain why elevation was the only terrain attribute with a significant positive effect on seedling survival within the BEF China in June 2010 in contrast to aspect, slope and curvature as reported by Yang *et al.* (2013). TRI does not affect soil acidity since this regional terrain attribute is predominately related to structural features of the surface like the spatial distribution of quartz veins and faults, as well as the duration of weathering and soil formation rather than erosion and landslides, which are better reflected by RR. However, minimum, maximum and mean soil pH of the upper 50 cm tend to slightly lower values of about 0.2 pH units at site B compared to site A (Fig. 2, online supplementary Table S2), which might reflect the higher degree of weathering at site B as well. The low CEC (about 56 $\mu mol_c\ g^{-1}$ soil) and percent BS (<20%) at both experimental sites result in small exchangeable Ca pools, and are indicative of only slightly weathered, young mineral soil. These soils might be highly sensitivity to intensive forest harvesting practices, if most nutrient rich biomass is removed (Federer *et al.* 1989). The small depth gradients of most terrain attributes correspond to this finding and support the important role of soil erosion on both experimental sites.

Soil fertility on both experimental sites can be regarded as low when following criteria given for soil survey and agricultural land evaluation in the subtropics and tropics (Landon 1991). The soils are very acid, the CEC is low to very low with little difference over all geomorphic units, and base cations are deficient. BS is <50% on all plots emphasizing dystric properties throughout the whole experimental area. With bulk densities below 1.4 g cm^{-3} the soils are not compacted indicating that the area of the experiment has not been cultivated recently. The Ca/Al ratio of the exchange complex on both experimental sites is below 0.2 on most plots and in accordance with the very low pH values (Gruba *et al.* 2013). This can cause inhibition of Ca uptake by tree roots and the very high Al saturation of the exchange complex probably indicate Al stress to fine roots influencing tree growth (De Wit *et al.* 2010; Kinraide 2003; Marschner 1991). However, the Ca/Al rations in foliage are higher than 12.5 in most cases and BS is less than 15 only on four single plots, especially on site B, and do not indicate adverse impacts on tree growth or nutrition in general (Cronan and Grigal 1995).

Tree growth is affected by soil fertility at small-scale

The main experiment of BEF China represents a random spatial configuration of diversity treatments projected onto a heterogeneous and complex real-world landscape. Because topography and soil fertility attributes vary at the same spatial scale as the plot dimension, which could be shown by a large number of significant correlations between topography and soil fertility attributes, it is difficult to isolate the

biotic signal from the environmental signal (Bruelheide *et al.* 2014; Healy *et al.* 2008). However, in the experimental framework of BEF China soil fertility and terrain affected tree height significantly (Table 4) after accounting for tree composition and tree species richness effects. Further interactions between biotic and abiotic control mechanisms were evident through altitudinal differences in survival rates of seedlings (Yang *et al.* 2013, 2017). Results from the mixed effects models for sapling growth responses at site A showed significant correlation to the local abiotic variables northness, N content and C/N ratio (Li *et al.* 2014a). However, Kröber *et al.* (2015) found only marginal effects of environmental variables on crown growth at site A, with slope being the best environmental predictor. According to our findings, soil C stocks were most closely related to tree height at this early stage of tree growth (1–2 years), whereas soil acidity, Mn and CEC were related to tree height only at site A. As trees at site A were planted 1 year earlier, we found more interactions between soil fertility and tree height growth at this experimental site. Soil acidification and high contents of exchangeable Al in the lower soil horizons could lead to restriction of nutrient uptake due to a poor replacement of base cations (Marschner 1991). Both nutrient deficiency and high Al contents can constrain fine root growth with soil depth, and cause a close dependence of tree growth on nutrient availability in topsoils, which showed higher C and N contents. Thus, plant nutrition most likely is coupled to a recycling of litter nutrients and root exudates rather than on supply of nutrients from the mineral soil and some trees might be able to bypass the common mineralization pathway by using a significant proportion of organic N as amino acids and proteins (Näsholm *et al.* 1998).

However, as shown before soil fertility was significantly affected by several terrain attributes and those additionally affect tree height. MCCA as indicator of water availability had a negative impact on tree growth, as well as the climatic terrain attribute northness showing the importance of irradiance for photosynthesis (see also Eichenberg *et al.* 2017). Planform curvature as a measure of soil erosion processes and matter transport showed that tree growth was reduced on very steep slopes. As tree heights varied more at site A, they also showed a relation to the geomorphological positions at which each tree grows. This again can be linked to erosion and accumulation processes along slopes in these two small catchments (Seitz *et al.* 2016). Generalized mixed-effects models showed that survival rates of tree seedlings were affected by species richness and negatively correlated to elevation (Yang *et al.* 2013). This can be explained by transport of base cations from ridge top and upper slopes downwards through interflow and erosion. Yang *et al.* (2017) found that tree richness did not affect shrub survival at this early stage of the experiment but single abiotic factors explained up to 5% of species survival, with a negative effect of slope inclination and a positive effect of the topsoil carbon to nitrogen ratio.

CONCLUSIONS

Our synthesis on the interrelation of soil fertility, topography and tree growth in a subtropical forest ecosystem in SE China showed that topographic heterogeneity led to ecological gradients across geomorphological positions. Although multilayered, the experimental design of BEF China with a high resolution of both terrain (5 m) and soil fertility attributes (approximately 25 m) allows to propose soil erosion and matter transport as key mechanisms for soil fertility and, thus, determine tree growth. Accordingly, we can confirm our first hypothesis. Our findings indicate low availability of exchangeable base cations and acid conditions in soils accompanied with high Al contents on both experimental sites, which could lead to limited tree growth due to insufficient soil nutrient supply. Especially plots on ridges and spurs may suffer both from nutrient leaching and from water shortage during dry and hot periods of the year. Such small-scale soil–plant interrelations in a young forest can serve as originator for the future development of vegetation and biodiversity control on soil properties in near-natural forest ecosystems. In addition, it showed that terrain attributes constitute an important predictor for the interpretation of soil fertility and tree growth in ecological research and it confirmed our second and third hypotheses that individual soil fertility variables are explained by terrain attributes and that tree growth is positively influenced by soil fertility, and thus also by terrain attributes. Nevertheless, in future years also the planted plot diversity may contribute to soil fertility besides topography.

SUPPLEMENTARY MATERIAL

Supplementary material is available at *Journal of Plant Ecology* online.

FUNDING

BEF-China is mainly funded by the German Research Foundation (DFG FOR 891/1, 2 and 3), with additional funds from the National Natural Science Foundation of China (NSFC 30710103907, 30930005, 31170457 and 31210103910), and the Swiss National Science Foundation (SNSF). We also benefitted from various travel grants and summer schools financed by the Sino-German Centre for Research Promotion in Beijing (GZ 524, 592, 698, 699 and 785) and the University of Tübingen, Germany (PROMOS).

ACKNOWLEDGEMENTS

We are indebted to the BEF-China students and team from China, Switzerland and Germany and their assistance in field and lab work, in particular to Susanne Nietzel, Jessica Henkner, Matthias Breitinger, Zhiqin Pei, Chen Lin, Christian Löffler, Sophie Schumacher, Susan Obst, Thomas Heinz, Kathrin Käppeler and all Chinese workers.
Conflict of interest statement. None declared.

REFERENCES

Ad-hoc-AG Boden (2005) *Bodenkundliche Kartieranleitung (5. Auflage)*. Hannover, Germany: E. Schweizerbart'sche Verlagsbuchhandlung.

Aldhous P (1993) Tropical deforestation: not just a problem in Amazonia. *Science* **259**:1390.

Anderson KE, Furley PA (1975) An assessment of the relationship between surface properties of chalk soils and slope form using principal component analysis. *J Soil Sci* **26**:130–43.

Baribault TW, Kobe RK, Finley AO (2012) Tropical tree growth is correlated with soil phosphorus, potassium, and calcium though not for legumes. *Ecol Monogr* **82**:189–203.

Behrens T (2003) *Digitale Reliefanalyse als Basis von Boden-Landschaftsmodellen am Beispiel der Modellierung Periglaziärer Lagen im Ostharz*. Giessen, Germany: Boden und Landschaft 15, Justus-Liebig-Universität Giessen.

Behrens T, Schmidt K, Ramirez-Lopez L, *et al*. (2014) Hyper-scale digital soil mapping and soil formation analysis. *Geoderma* **213**:578–88.

Behrens T, Schmidt K, Scholten T (2008) An approach to removing uncertainities in nominal environmental covariates and soil class maps. In Hartemink A, McBratney A, Mendosa–Santos ML (eds). *Digital Soil Mapping With Limited Data*. Berlin, Germany: Springer, 213–24.

Behrens T, Schmidt K, Zhu A-X, *et al*. (2010a) The ConMap approach for terrain-based digital soil mapping. *Europ J Soil Sci* **61**:133–43.

Behrens T, Zhu A-X, Schmidt K, *et al*. (2010b) Multi-scale digital terrain analysis and feature selection for digital soil mapping. *Geoderma* **155**:175–85.

Blasch G, Spengler D, Hohmann C, *et al*. (2015) Multitemporal soil pattern analysis with multispectral remote sensing data at the field-scale. *Comput Electron Agr* **113**:1–13.

Bormann FH, Likens GE (1966) Comparative nutrient losses in solution and in particulate matter from an undisturbed northern hardwood ecosystem. *Bull Ecol Soc Amer* **47**:115.

Boyden S, Montgomery R, Reich PB, *et al*. (2012) Seeing the forest for the heterogeneous trees: stand-scale resource distributions emerge from tree-scale structure. *Ecol Appl* **22**:1578–88.

Breiman L (2001) Random forests. *Mach Learn* **45**:5–32.

Bruelheide H, Böhnke M, Both S, *et al*. (2011) Community assembly during secondary forest succession in a Chinese subtropical forest. *Ecol Monogr* **81**:25–41.

Bruelheide H, Nadrowski K, Assmann T, *et al*. (2014) Designing forest biodiversity experiments: general considerations illustrated by a new large experiment in subtropical China. *Methods Ecol Evol* **5**:74–89.

Bu WS, Schmid B, Liu XJ, *et al*. (2017) Interspecific and intraspecific variation in specific root length drives aboveground biodiversity effects in young experimental forest stands. *J Plant Ecol* **10**:158–69.

Burnett MR, August P, Brown JH, *et al*. (1998) The influence of geomorphological heterogeneity on biodiversity I. A patch scale perspective. *Conserv Biol* **12**:363–70.

Butler D (2009) *Asreml: Asreml Fits the Linear Mixed Model. Software R Package Version 3.0*. Hemel Hempstead, UK: VSN International Ltd.

Cardinale BJ, Matulich KL, Hooper DU, *et al*. (2011) The functional role of producer diversity in ecosystems. *Am J Bot* **98**:572–92.

Chen HY, Klinka K, Kabzems RD (1998) Site index, site quality, and foliar nutrients of trembling aspen: relationships and predictions. *Can J Forest Res* **28**:1743–55.

Clemens G, Fiedler S, Nguyen DC, *et al*. (2010) Soil fertility affected by land use history, relief position, and parent material under a tropical climate in NW-Vietnam. *Catena* **81**:87–96.

Cronan CS, Grigal DF (1995) Use of calcium/aluminum ratios as indicators of stress in forest ecosystems. *J Environ Qual* **24**:209–26.

De Wit HA, Eldhuset TD, Mulder J (2010) Dissolved Al reduces Mg uptake in Norway spruce forest: results from a long-term field manipulation experiment in Norway. *Forest Ecol Manag* **259**:2072–82.

Don A, Scholten T, Schulze ED (2009) Conversion of cropland into grassland: implications for soil organic carbon stocks in two soils with different texture. *J Plant Nutr Soil Sci* **172**:53–62.

Eichenberg D, Pietsch K, Meister C, *et al*. (2017) The effect of microclimate on wood decay is indirectly altered by tree species diversity in a litterbag study. *J Plant Ecol* **10**:170–8.

Enoki T, Kawaguchi H (2000) Initial nitrogen content and topographic moisture effects on the decomposition of pine needles. *Ecol Res* **15**:425–34.

Federer CA, Hornbeck JW, Tritton LM, Robert WM, Smith CT (1989) Long-term depletion of calcium and other nutrients in eastern US forests. *Environ Manage* **13**:593–601.

Forrester DI (2014) The spatial and temporal dynamics of species interactions in mixed-species forests: from pattern to process. *Forest Ecol Manag* **312**:282–92.

Forrester DI, Cowie AL, Bauhus J, *et al*. (2006) Effect of changing the supply of nitrogen and phosphorous on growth and interaction between *Eucalyptus globulus and Acacia mearnsiiin* in a pot trial. *Plant Soil* **280**:267–77.

Frank DA, Pontes AW, McFarlane KJ (2012) Controls on soil organic carbon stocks and turnover among North American ecosystems. *Ecosystems* **15**:604–15.

Gao C, Zhang Y, Shi N-N, *et al*. (2015) Decreasing influence of contemporary environment on the ectomycorrhizal fungal communities along a secondary succession in a Chinese subtropical forest. *New Phytologist* **205**:771–85.

Giaccio B, Galadini F, Spasato A, *et al*. (2002) Image processing and roughness analysis of exposed bedrock fault planes as a tool for paleoseismological analysis: results from the Campo Felice fault (central Apennines, Italy). *Geomorphology* **49**:281–301.

Glinka KD (1927) *Dokuchaiev's Ideas in the Development of Pedology and Cognate Sciences*. Moscow, Russia: U.S.S.R. Acad. Sci. Russian Pedological Investigations I.

Goebes P, Seitz S, Kühn P, *et al*. (2015a) Throughfall kinetic energy in young subtropical forest: investigation on tree species richness effects and spatial variability. *Agr Forest Meteorol* **213**:148–59.

Goebes P, Bruelheide H, Härdtle W, *et al*. (2015b) Species-specific effects on throughfall kinetic energy in subtropical forest plantations are related to leaf traits and tree architecture. *PLOS ONE* **10**:e0128084.

Gosz JR, Likens GE, Bormann FH (1973) Nutrient release from decomposing leaf and branch litter in Hubbard Brook forest, New-Hampshire. *Ecol Monogr* **43**:173–91.

Griffiths RP, Madritch MD, Swanson AK (2009) The effects of topography on forest soil characteristics in the Oregon Cascade Mountains

(USA): implications for the effects of climate change on soil properties. *Forest Ecol Manage* **257**:1–7.

Gruba P, Mulder J, Brożek S (2013) Modelling the pH dependency of dissolved calcium and aluminium in O, A and B horizons of acid forest soils. *Geoderma* **206**:85–91.

Gu XX, Liu JM, Zheng MH, *et al*. (2002) Provenance and tectonic setting of the proterozoic turbidites in Hunan, South China: geochemical evidence. *J Sediment Res* **72**:393–407.

Hairston AB, Grigal DF (1991) Topographic influences on soils and trees within single mapping units on a sandy outwash landscape. *Forest Ecol Manage* **43**:35–45.

Healy C, Gotelli NJ, Potvin C (2008) Partitioning the effects of biodiversity and environmental heterogeneity for productivity and mortality in a tropical tree plantation. *J Ecol* **96**:903–13.

Hilgard EW (1914) *Soils*. New York, NY: The Macmillan Company.

Homeier J, Breckle SW, Guenter S, *et al*. (2010) Tree diversity, forest structure and productivity along altitudinal and topographical gradients in a species-rich Ecuadorian montane rain forest. *Biotropica* **42**:140–8.

Huang BW (1987) Slopeland utilization and amelioration: importance and feasibility. *Geogr Res* **6**:1–15.

Hugget JR (1975) Soil landscape systems: a model of soil genesis. *Geoderma* **13**:1–22.

Huntington TG (2003) Calcium depletion in forest soils. In Lal R (ed). *Encyclopedia of Soil Science*. New York, NY: Marcel Dekker.

IUSS Working Group WRB (2014) *World Reference Base for Soil Resources 2014, International Soil Classification System for Naming Soils and Creating Legends for Soil Maps*. World Soil Resources Reports 103. FAO, Rome.

Jasiewicz J, Stepinski TF (2013) Geomorphons — a pattern recognition approach to classification and mapping of landforms. *Geomorphology* **182**:147–56.

Jenny H (1941) *Factors of Soil Formation: A System of Quantitative Pedology*. New York, NY: McGraw Hill.

Jien SH, Lee MH, Hseu ZY, *et al*. (2015) Erosion potential estimation by network measurement of soil properties in coastal areas after clearcutting. *Int J Distrib Sens N* **2015**:281321.

Kinraide TB (2003) Toxicity factors in acid forest soils: attempts to evaluate separately the toxic effects of excessive Al^{3+} and H^{+} and insufficient Ca^{2+} and Mg^{2+} upon root elongation. *Eur J Soil Sci* **54**:323–33.

Krige DG (1951) A statistical approach to some basic mine valuation problems on the Witwatersrand. *J Chem Metall Min Soc S Af* **52**:119–39.

Kröber W, Li Y, Härdtle W, *et al*. (2015) Early subtropical forest growth is driven by community mean trait values and functional diversity rather than the abiotic environment. *Ecol Evol* **5**:3541–56.

Landon JR (ed) (1991) *Booker Tropical Soil Manual: A Handbook for Soil Survey and Agricultural Land Evaluation in the Tropics and Subtropics*. New York, NY: Longman-Wiley, 474.

Legendre P, Mi XC, Ren HB, *et al*. (2009) Partitioning beta diversity in a subtropical broad-leaved forest of China. *Ecology* **90**:663–74.

Li Y, Härdtle W, Bruelheide H, *et al*. (2014a) Site and neighborhood effects on growth of tree saplings in subtropical plantations (China). *Forest Ecol Manag* **327**:118–27.

Li Y, Hess C, von Wehrden H, *et al*. (2014b) Assessing tree dendrometrics in young regenerating plantations using terrestrial laser scanning. *Ann For Sci* **71**:453–62.

Li Y, Kröber W, Bruelheide H, *et al*. (2017) Crown and leaf traits as predictors of subtropical tree sapling growth rates. *J Plant Ecol* **10**:136–45.

Liaw A, Wiener M (2002) Classification and regression by random forest. *R News* **2**:18–22.

Likens GE, Driscoll CT, Buso DC (1996) Long-term effects of acid rain: response and recovery of a forest ecosystem. *Science* **272**:244–6.

Marschner H (1991) Mechanisms of adaptation of plants to acid soils. *Plant Soil* **134**:1–20.

Matzner E, Ulrich B (1981) Balances of annual element fluxes within forest ecosystems in the Solling region. *J Plant Nutr Soil Sc* **144**:660–81.

McBratney AB, Mendonca-Santos ML, Minasny B (2003) On digital soil mapping. *Geoderma* **12**:3–52.

McKenney DW, Pedlar JH (2003) Spatial models of site index based on climate and soil properties for two boreal tree species in Ontario, Canada. *Forest Ecol Manag* **175**:497–507.

McNab WH (1989) Terrain shape index: quantifying effect of minor landforms on tree height. *Forest Sci* **35**:91–104.

Milne G (1935) Some suggested units of classification and mapping particularly for East African soils. *Soil Res* **4**:183–98.

Näsholm T, Ekblad A, Nordin A, *et al*. (1998) Boreal forest plants take up organic nitrogen. *Nature* **392**:914–6.

Nadrowski K, Wirth C, Scherer-Lorenzen M (2010) Is forest diversity driving ecosystem function and service? *Current Opin Environ Sustain* **2**:75–9.

Nanko K, Giambelucca TW, Sutherland RA, *et al*. (2015) Erosion potential under Miconia Calvescens stands on the island of Hawai'i. *Land Degrad Develop* **26**:218–26.

Officer SJ, Kravchenko A, Bollero GA, *et al*. (2004) Relationships between soil bulk electrical conductivity and the principal component analysis of topography and soil fertility values. *Plant Soil* **258**:269–80.

O'Loughlin EM (1973) Saturation regions in catchments and their relationship to soil and topographic properties. *J Hydrol* **53**:229–46.

Pacès T (1985) Sources of acidification in Central Europe estimated from elemental budgets in small catchments. *Nature* **315**:31–6.

Patzel N, Sticher H, Karlen DL (2000) Soil fertility — phenomenon and concept. *J Plant Nutr Soil Sci* **163**:129–42.

Peng SY, Schmid B, Haase J, *et al*. (2017) Leaf area increases with species richness in young experimental stands of subtropical trees. *J Plant Ecol* **10**:128–35.

Pennock DJ, Zebarth BJ, De Jong E (1987) Landform classification and soil distribution in hummocky terrain, Saskatchewan, Canada. *Geoderma* **40**:297–315.

Perakis SS, Maguire DA, Bullen TD, *et al*. (2006) Coupled nitrogen and calcium cycles in forests of the Oregon coast range. *Ecosystems* **9**:63–74.

Poszwa A, Dambrine E, Pollier B, Atteia O (2000) A comparison between Ca and Sr cycling in forest ecosystems. *Plant and Soil* **225**:299–310.

Pretzsch H, Dieler J (2011) The dependency of the size-growth relationship of Norway spruce (*Picea abies* [L.] Karst.) and European beech (*Fagus sylvatica*[L.]) in forest stands on long-term site conditions, drought events, and ozone stress. *Trees* **25**:355–69.

Qin C-Z, Zhu A-X, Pei T, *et al*. (2011) An approach to computing topographic wetness index based on maximum downslope gradient. *Precis Agric* **12**:32–43.

R Development Core Team (2013) *R: A Language and Environment for Statistical Computing*. Vienna, Austria: R Foundation for Statistical Computing.

Riedel J, Dorn S, Plath M, *et al*. (2013) Time matters: temporally changing effects of planting schemes and insecticide treatment on native timber tree performance on former pasture. *For Ecol Manag* **297**:49–56.

Riley SJ, De Gloria SD, Elliot R (1999) A terrain ruggedness that quantifies topographic heterogeneity. *Intermount J Sci* **5**:23–7.

Roberts DW (1986) Ordination on the basis of fuzzy set theory. *Vegetatio* **66**:123–31.

Rossel RAV, Rizzo R, Dematte JAM, *et al*. (2010) Spatial modeling of a soil fertility index using visible-near-infrared spectra and terrain attributes. *Soil Sci Soc Am J* **74**:1293–300.

Scherer-Lorenzen M (2014) The functional role of biodiversity in the context of global change. In Burslem D, Coomes D, Simonson W (eds). *Forests and Global Change*. Cambridge, UK: Cambridge University Press, 195–238.

Schmidt K, Behrens T, Scholten T (2008) Instance selection and classification tree analysis for large spatial datasets in digital soil mapping. *Geoderma* **146**:138–46.

Schmidt K, Behrens T, Scholten T (2009) A method to generate soilscapes from soil maps. *J Plant Nutr Soil Sc* **173**:163–72.

Schönbrodt S, Behrens T, Schmidt K, *et al*. (2013) Degradation of cultivated bench terraces in the Three Gorges Area: field mapping and data mining. *Ecol Indic* **34**:478–93.

Scholten T, Felix-Henningsen P, Schotte M (1997) Geology, soils and saprolites of the Swaziland Middleveld. *Soil Technology* **11**:229–46.

Seitz S, Goebes P, Song Z, *et al*. (2016) Tree species identity and canopy characteristics but not species richness affect interrill soil erosion processes in young subtropical forests. *Soil* **2**:649–61.

Seitz S, Goebes P, Zumstein P, *et al*. (2015) The influence of leaf litter diversity and soil fauna on initial soil erosion in subtropical forests. *Earth Surf Proc Land* **40**:1439–47.

Shu LS, Charvet J (1996) Kinematics and geochronology of the Proterozoic Dongxiang-Shexiang ductile hear zone with HP metamorphism a and ophiolitic melange (Jiangnan Region, South China). *Tectonophysics* **267**:291–302.

Stille P, Pierret MC, Steinmann M, *et al*. (2009) Impact of atmospheric deposition, biogeochemical cycling and water-mineral interaction on REE fractionation in acidic surface soils and soil water (the Strengbach case). *Chem Geol* **264**:173–86.

Sun ZK, Liu XJ, Schmid B, *et al*. (2017) Positive effects of tree species richness on fine-root production in a subtropical forest in SE-China. *J Plant Ecol* **10**:146–57.

Tarboton DG (1997) A new method for the determination of flow directions and upslope areas in grid digital elevation models. *Water Resour Res* **33**:309–19.

Tilman D, Isbell F, Cowles JM (2014) Biodiversity and ecosystem functioning. *Annu Rev Ecol Evol System* **45**:471–93.

van Breugel M, Hall JS, Craven DJ, *et al*. (2011) Early growth and survival of 49 tropical tree species across sites differing in soil fertility and rainfall in Panama. *For Ecol Manag* **261**:1580–9.

Wang H, Liu SR, Mo JM, *et al*. (2010) Soil organic carbon stock and chemical composition in four plantations of indigenous tree species in subtropical China. *Ecol Res* **25**:1071–9.

Wang K, Shi X-Z, Yu D-S, *et al*. (2005) Environmental factors affecting temporal and spatial dynamics of soil erosion in Xingguo county, South China. *Pedosphere* **15**:620–7.

Wezel A, Steinmuller N, Friederichsen JR (2002) Slope position effects on soil fertility and crop productivity and implications for soil conservation in upland northwest Vietnam. *Agric Ecosyst Environ* **91**:113–26.

Wu H (2015) The relationship between terrain factors and spatial variability of soil nutrients for pine-oak mixed forest in Qinling Mountains. *J Nat Res* **30**:858–69.

Wu YT, Gutknecht J, Nadrowski K, *et al*. (2012) Relationships between soil microorganisms, plant communities, and soil characteristics in Chinese subtropical forests. *Ecosystems* **15**:624–36.

Wu YT, Wubet T, Trogisch S, *et al*. (2013) Forest age and plant species composition determine the soil fungal community structure in a Chinese subtropical forest. *PLOS ONE* **8**:e66829.

Wood TE, Lawrence D, Clark DA (2006) Determinants of leaf litter nutrient cycling in a tropical rain forest: soil fertility versus topography. *Ecosystems* **9**:700–10.

Xiao W, He H (2005) Early Mesozoic thrust tectonics of the northwest Zhejiang region (Southeast China). *Geol Soc Am Bull* **117**:945–61.

Xie Z, Zhu J, Gang L, *et al*. (2007) Soil organic carbon stocks in China and changes from 1980s to 2000s. *Glob Change Biol* **13**:1989–2007.

Xue L, Xue Y, Lie GW, *et al*. (2012) Soil organic carbon storacge on different slope positions in *Cunninghamia Lanceolata* stands. *Bull Soil Water Conserv* **32**:43–6.

Yang B, Li Y, Ding BY, *et al*. (2017) Impact of tree diversity and environmental conditions on the survival of shrub species in a forest biodiversity experiment in subtropical China. *J Plant Ecol* **10**:179–89.

Yang X, Bauhus J, Both S, *et al*. (2013) Establishment success in a forest biodiversity and ecosystem functioning experiment in subtropical China (BEF-China). *Eur J Forest Res* **132**:593–606.

Yokoyama R, Shirasawa M, Pike RJ (2002) Visualizing topography by openness: a new application of image processing to digital elevation models. *Photogramm Eng Rem S* **68**:257–65.

Zhang J, Ge Y, Chang J, *et al*. (2007) Carbon storage by ecological service forests in Zhejiang Province, subtropical China. *Forest Ecol Manag* **245**:88–95.

Zhang N, Wang XH, Zheng ZM, *et al*. (2012) Spatial heterogeneity of soil properties and its relationships with terrain factors in broadleaved forest in Tiantong of Zhejiang Province, East China. *Chin J Appl Ecol* **23**:2361–9.

Zevenbergen LW, Thorne CR (1987) Quantitative analysis of land surface topography. *Earth Sur Proc Land* **12**:47–56.